Available online www.jocpr.com

Journal of Chemical and Pharmaceutical Research, 2016, 8(8):749-757

Research Article

ISSN : 0975-7384
CODEN(USA) : JCPRC5

Optical and dielectric behavior of NiO: Zn quantum dots

C. Thangamani and K. Pushpanathan*

Nanomaterials Research Laboratory, Department of Physics, Government Arts College, Karur - 639 005. India

ABSTRACT

Present study focuses the synthesis and characterization of undoped and zinc doped nickel oxide nanoparticles. Prepared nanopowders have been characterized by means of x-ray diffraction method, high-resolution scanning electron microscope, ultraviolet visible spectrometer, photoluminescence spectrometer, Fourier transform infrared spectrometer, impedance meter, and thermal gravimetric analyzer. X - ray diffraction analysis confirmed the average crystalline size of the nanopowder is less than 20 nm. Ultraviolet-visible spectrometer recorded the absorption peaks between 336 - 346 nm, corresponding to the energy gap of 3.70 – 3.58 eV. Photoluminescence spectrometer showed the near band edge emission. Fourier transform infrared spectroscopy analysis confirmed the formation of the nickel oxide and the zinc dopant. The high-resolution scanning electron microscope image depicts that the particles are uniform in size and they are in severe agglomeration. The dielectric studies established the decrease in dielectric losses with increasing the temperature as well as frequency. Thermo gravimetric study shows that the prepared samples have good stability.

Key words: NiO nanoparticles; Crystal structure; Microstructure; Energy gap; Photoluminescence.

INTRODUCTION

Recently nanostructured semiconductor metal oxides are gradually gaining attention due to its extraordinary optical properties [1, 2]. Many researches are working in divalent metal-doped nickel oxide (NiO) nanoparticle for a wide range of applications. Certainly, NiO is one of the promising and environment friendly *p-type* semiconductors with wide band gap energy ranging from 3.6 to 4 eV (bulk form). It is extensively used in many areas *such as* sensing devices, chemical micro sensors, gas sensors, agriculture, spintronic devices, superconductors, solar cells and anti-ferromagnetic layers, quantum tunneling, exchange coupled dynamics, and optical coating [3- 4]. In addition, NiO nanomaterials are having excellent thermal stability, which makes them suitable for microelectronics and electro chromic material for display [5-6]. It is reported that the electrical conductivity of NiO is depending on the formation of microstructural defects, due to nickel vacancies and interstitial oxygen in NiO crystallites [7]. Stoichiometric NiO is a Mott insulator but one can increase its p-type conductivity by doping an ion with positive charge [8] and also by thermal treatment. Few Ni^{2+} ions becomes Ni^{3+} oxidation compensation and thus acquires on excess oxygen becomes slightly non-stoichiometric and Ni vacancies are trapped by Ni^{3+} ions in the ground state [9].

There are few reports on synthesis and characterization of Zn doped NiO nanoparticles. For instance, Sathishkumar *et. al.*,[10] investigated the structural, magnetic and electrochemical properties of Zn doped NiO nanocrystals by chemical precipitation method at room temperature. They observed that Zn doped NiO can be used in electrode material for the supercapacitor application. Karthik *et. al.*,[11] have found that the band gap energy Eg of NiO is 2.93 eV. The increase in band gap energy of NiO nanoparticles is the indicative of the quantum confinement effect and arising from the tiny crystallites. Gokul *et. al.*,[12]reported that NiO nanoparticles possess negative temperature coefficient resistance and the *ac* and *dc* conductivities depends on the temperature and the particles. In similar fashion, Marlick et. *al.*,[13] investigated the activation energy and frequency of NiO and Fe doped NiO, and they found that the activation energy and frequency depending on electrical conductivity. They measured the activation

energy of NiO and Fe doped NiO is 0.51 and 0.85 eV, respectively. Further they noticed that by increasing the dopant concentration the activation energy can be increased, due to solubility restrictions. Ramasubba Reddy *et. al.*,[14] found that the Raman peak presented at 518 cm^{-1} confirms Ni-O bands and no impurity peaks were presented due to Cu dopant. Giant dielectric resonance has been identified in divalent metal ion doped NiO ceramics. Mallick *et. al.,* [15] reported that the evolution of structure, microstructure, electrical, and magnetic properties of NiO with divalent metal ion doping. They observed that the crystal structure is not affected by the divalent substitution, but microstructure is affected.

The fundamental property of nanoparticles is seeing that their structure, particle size, distribution, and morphology are nearly related to the preparation techniques. Various synthesis methods have been developed to prepare nanoparticles. For example, sol-gel method, solvothermal method, electrochemical routes, hydrothermal reaction, and chemical precipitation method are the most common method of preparing the nanoparticles. Here, we have chosen the chemical precipitation method for the present study. Compared to other method this is very simplest method, low cost, easy to prepare the nanoparticles with low temperatures, easy to produce the particle and to control the particle size [16].

This article mainly focuses the synthesis and characterization of undoped and Zn doped NiO quantum dots *via* chemical precipitation method at different Zn concentration. Structural, optical, morphological, photoluminescence, dielectric behavior and thermal stability of the prepared samples have been studied.

EXPERIMENTAL SECTION

Synthesis of undoped NiO and Zn doped NiO nanopowder

Undoped and Zn doped NiO nanoparticles were successfully synthesized by an simple precipitation method using analytical grade nickel acetate di-hydrate [Ni $(CH_3COOH)_2 \cdot 2H_2O$ 99.5%, Merck], zinc acetate [$Zn(CH_3COOH)_2$, 99.7% purity] and sodium hydroxide (NaOH, Merck, 99.5% purity). These chemicals were used without further purification.

For the synthesis of NiO sample, 200 mL of 0.5 M nickel acetate di-hydrate solution was taken in a beaker. With this solution, required amount of sodium hydroxide (NaOH) pellets were dropped directly in the solution so as to reach the pH of the solution 12. The light green solution obtained so it was stirred with magnetic stirrer for 3 hours. Following this,2 ml of Polyethylene glycol (PEG MW: 400) was added as a capping agent to the mixture of nickel acetate and sodium hydroxide solution and the same was kept in an airtight container for a two days towards the slow crystallization. Consequently, NiO precipitation settled down at the bottom of the beaker. Then the sodium acetate [Na (CH_3COO)] transparent solution was removed and the particles were washed with distilled water and ethanol several times to remove the unreacted components.

Similar procedure was followed for the synthesis of Zn doped NiO ($Ni_{1-x}Zn_xO$ where x = 0.01, 0.03 and 0.05) samples and then the particles thus obtained was filtered and dried at 100˚C for 2 hours in a hot air oven to remove the remaining water content from the sample. Finally all the four samples have been annealed at 300˚C for 3 hours.

Characterization

The prepared sample crystalline nature was acknowledged using Philips Analytical X-ray diffractometer (Model No. PW1830) equipped with Ni filtered CuKα radiation (λ = 0.154187 nm) for 2θ = 30 - 80˚, with scanning rate of "5˚" min^{-1}" operated at 40 kV/30 mA. Surface morphology and elemental information of the samples were examined by using high-resolution scanning electron microscope (HRSEM- FEI Quanta FEG 200). JEOL-2100 transmission electron microscope (TEM) was used to confirm the microstructure and size. The absorption and transmittance properties were studied by using Lambda 35 (PERKINELMER: USA) Ultraviolet-visible (UV-Vis) spectrophotometer. The functional group of the synthesized undoped and Zn doped NiO nanostructures were characterized by the fourier transform infrared (FTIR) spectroscopy in the range of 4000 – 400 cm^{-1}. The photoluminescence (PL) measurements were carried out at room temperature by means of PL spectrometer (Kimon, SPEC-14031K, Japan) with a He-Cd laser line of 325 nm as the excitation source. Dielectric measurements were characterized by using LCR HiTESTER impedance meter at different temperature. Thermo gravimetric and differential thermo gravimetric analysis has been carried out (NETZSCH STA 449F3) in N_2 atmosphere.

RESULTS AND DISCUSSION

Structural analysis

The phase composition, purity and structure of the prepared nanoparticles were examined by x-ray diffraction (XRD) method. Figure 1 shows the x- ray diffraction pattern of $Ni_{1-x}Zn_xO$ (where x = 0, 0.01, 0.03 and 0.05) nanoparticles recorded at room temperature. These peaks at the scattering angles (2θ) of 37.16°, 43.29°, 62.8°, 75.24° and 79.43° correspond to the reflection planes (222), (400), (440), (622) and (444) of NiO crystal, respectively.

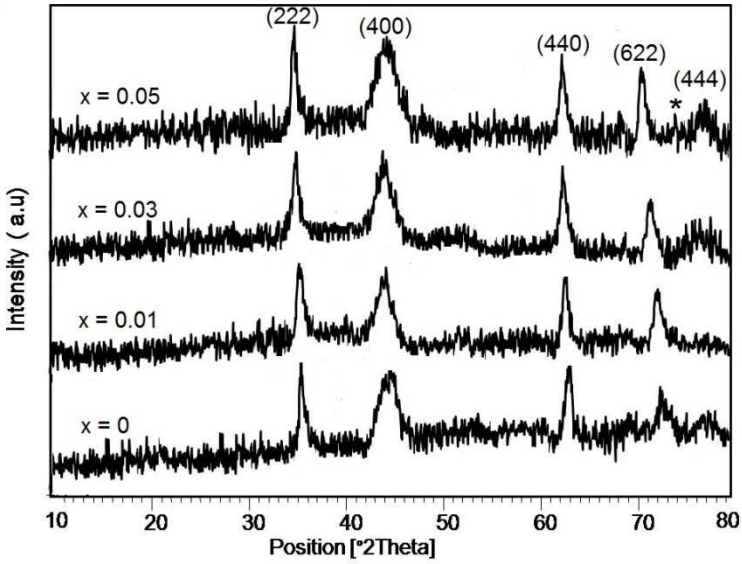

Figure 1. X-ray diffraction pattern of the $Ni_{1-x}Zn_xO$ (x= 0, 0.01, 0.03, and 0.05) nanopowders annealed at 300 ˚C for 3 hrs show that the crystal structure of the samples is cubic till x = 0.01 thereafter impurity phase arises

From the XRD pattern, it is clear that until x = 0.01 there is no other characteristic peaks, such as nickel, zinc or zinc oxide, can be detected, indicating that a single face centered cubic structure was obtained using this precipitation method. All diffraction peaks agreed with (JCPDS CARD 89-5881). Further increase in x to 0.03 and 0.05, a less intense peak has been observed which is marked by the * symbol. The high intensity peak (400) has been used to estimate the average crystalline size (D) of sample with the help of Scherer equation and the lattice constant $d_{(hkl)}$.

$$D = \frac{0.9\lambda}{\beta Cos\theta}$$

$$d_{(hkl)} = \frac{a}{\sqrt{(h+k+l)}}$$

Where D is the mean grain size, λ is the x-ray wavelength (for Cu Kα radiation, λ = 1.541 Å), θ is the diffraction angle, β is the full width at half maximum (FWHM) and $d_{(hkl)}$ is the interplanar distance collected from the XRD result. The average crystalline size of the undoped NiO nanoparticle is 11 nm and it was found to increase to 18.8 nm with increasing Zn concentration to 5(wt %).

The lattice constant calculated to be 'a' = ~ 8.330 Å for NiO and it increases to 8.353 Å for 5% Zn doped NiO nanopowder. Unit cell volume (V) has been calculated using the equation $V = a^3$ and it increases from 578 to 582.81(Å) ^{3}. All these premeditated parameters are listed in table 1. The increase in lattice constant and unit cell volume may be due to the substitution of Zn^{2+} ion with larger ionic radius of 0.74 Å in place of Ni^{2+} (0.69 Å) ion. We also noticed from the data in table 1, that there is about 0.83% increase in the unit cell volume as the lattice constant increases from 8.330 to 8.353 Å. Further, the XRD profile shows that NiO nanoparticles are strongly crystallized with a preferred (400) orientation, which has been observed by other authors [17,18]. The dislocation density 'S' is a measure of amount of defects and vacancies in the crystal which can be determined from the particle size "D" using the formula

$$S = \frac{1}{D^2}$$

It can be seen from the table 1 that S decreasing from 8.2 x 10^{15} to 2.8 x 10^{15} with increasing Zn concentration. It indicates that the lattice imperfection decreases with particle size. Similarly, micro-strain (ε) can also be calculated using the formula

$$\text{Micro-strain} = \frac{\beta \cos\theta}{4}$$

Table 1: Crystalline size, lattice parameter, unit cell volume undoped and Zn doped NiO nanoparticles

Sample	Average crystalline size (nm)	Lattice constant '*a*' (Å)	Unit cell volume '*V*' $(Å)^3$	Micro strain (ε) x 10^{-3}	Dislocation Density (S) 10^{15}
NiO	11.06	8.330	578.00	3.2	8.2
$Ni_{0.99}Zn_{0.01}O$	13.80	8.338	579.68	4.0	5.3
$Ni_{0.97}Zn_{0.03}O$	16.21	8.350	582.18	3.2	3.8
$Ni_{0.95}Zn_{0.05}O$	18.84	8.353	582.81	7.2	2.8

It has been observed that the micro-strain is increased from 3.2 x 10^{-3} to 7.2 x 10^{-3} as the Zn concentration is increased from 0 to 5 (wt%). In general, variation in micro-strain may be due to the change in microstructure, size and shape of the particles. Figure 2(a&b) depicts the variation grain size vs. Zn content and variation of lattice constant and unit cell volume of the NiO:Zn nanoparticles.

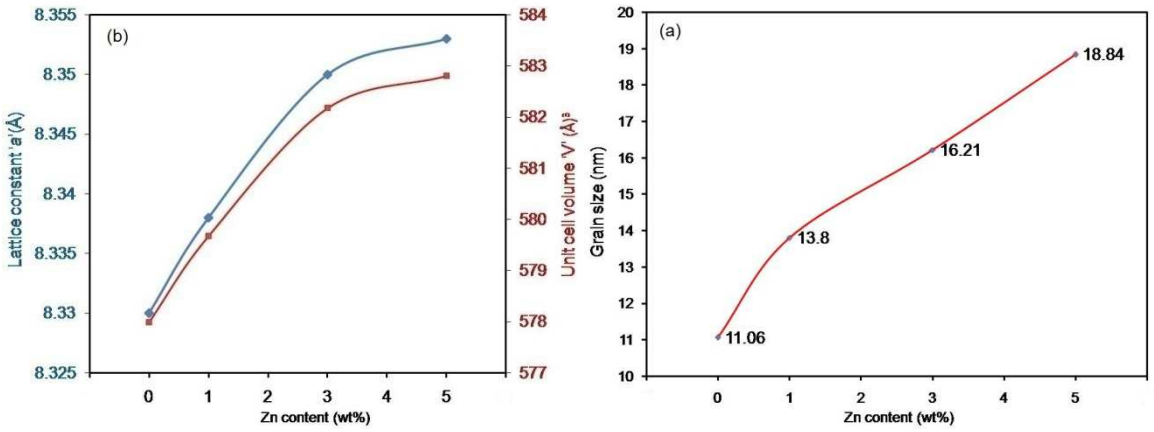

Figure 2. Variation of (a) grain size vs. Zn content and (b) lattice constant and unit cell volume vs. Zn content of the nanoparticles

UV –Visible analysis

The UV-visible absorption spectroscopy is one of the very important techniques to find the band gap. In our study, the optical absorption spectra of undoped and Zn doped NiO samples between 250 nm to 550 nm were recorded and the same is presented in Figure 3. It can be seen that the absorption (λ_{ab}) increases from 336 to 346 nm as *x* increases from 0 to 5 (wt%).

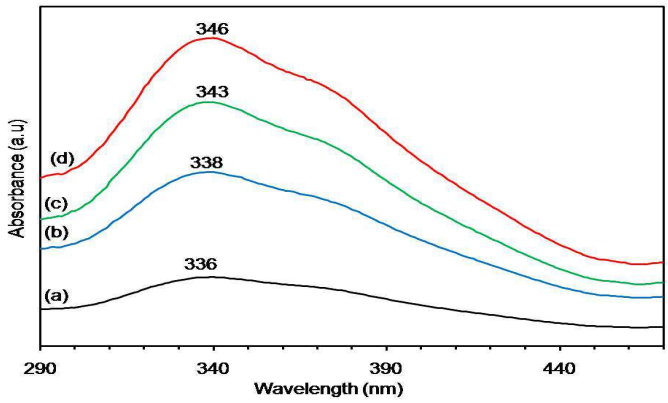

Figure 3. UV-Vis absorption spectrum of the synthesized $Ni_{1-x}Zn_xO$ nanopowders: (a) *x* = 0, (b) *x* = 0.01, (c) *x* = 0.03, and (d) *x* = 0.05

Energy gap of the prepared nanoparticles has been calculated from the formula $E_g = (1240/\lambda_{ab})$ and it is found to be 3.70 eV for NiO and 3.58 eV for $Ni_{0.95}Zn_{0.05}O$. Table 2 summarizes the energy gap variation vs. Zn^{2+} ion concentration. Here, the E_g of $Ni_{0.95}Zn_{0.05}O$ is lower than that of bulk NiO, which correspond the blue shift in the spectrum. This confirms the quantum confinement effect in NiO nanoparticles and Zn doped NiO nanoparticles. Energy gap reported here matches well with the previous work [19].

Table 2: Energy gap variation vs. Zn^{2+} ion concentration

Sample	Zn concentration (*x*)	Absorption peak (nm)	Energy gap (eV)
$Ni_{1-x}Zn_xO$	0.00	336	3.70
	0.01	338	3.67
	0.03	343	3.62
	0.05	346	3.58

FT-IR analysis

Figure 4 shows the FTIR spectra of undoped and Zn doped NiO nanoparticles recorded in the range of 4000 to 400 cm^{-1}. The peak observed at 3641 cm^{-1} for undoped NiO and 3635 cm^{-1} for 5(wt%) Zn doped NiO nanoparticles are attributed to the O-H stretching vibrations of water molecules present in the sample [20]. The another absorption band centered at ~2826 cm^{-1} of NiO and 2085 cm^{-1} for Zn dopant NiO samples are associated with C-H stretching mode on the surface of the products [21]. In addition to this, the peaks at 1639 cm^{-1}, 1633 cm^{-1} is attributed to the O-H-O bending vibration modes. The bands appearing at 1471 cm^{-1}, 1023 cm^{-1} are assigned to the presence of carbonates. Finally, the presence of NiO and Zn doped NiO nanoparticles are confirmed by the absorption peaks at 515 cm^{-1}, 510 cm^{-1}. The broadness of Ni-O stretching vibration mode and Zn doped NiO vibration modes identify that the synthesized samples are pure. Finally, from FTIR spectrum, it is concluded that the frequency shift from lower wave number to higher wave number is due to the increasing the Zn concentration.

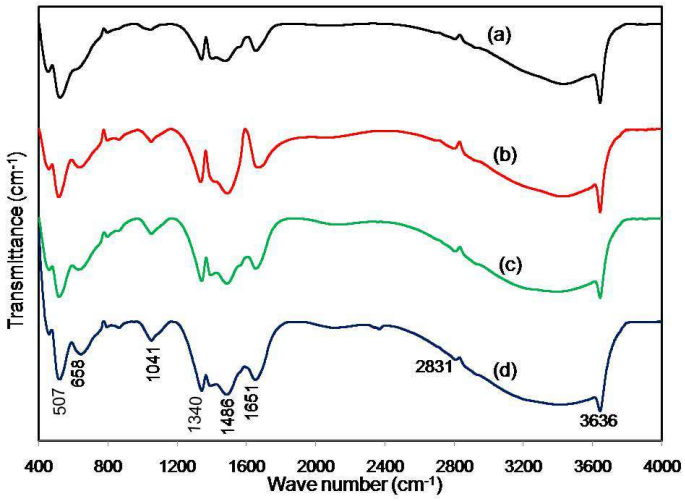

Figure 4. FTIR spectra of of the synthesized nanopowders: (a) NiO, (b) $Ni_{0.99}Zn_{0.01}O$, (c) $Ni_{0.97}Zn_{0.03}O$, and (d) $Ni_{0.95}Zn_{0.05}O$

Photoluminescence (PL) analysis

The room temperature photoluminescence spectra of undoped and Zn doped NiO nanoparticles are shown in figure 5. It can be seen that the intensity only varies whereas no change in the position of the peak. Moreover, the spectrum consists of four different emissions. The emission at 355 nm, corresponds the energy gap of 3.5 eV, is the characteristic emission peak of NiO nanoparticles. Then, the violet emission at 410 nm and blue emission at 490 nm are weak. These weak emissions are the result of near band edge emission. Two strong shoulder peak observed at 520 nm to 538 nm are represents the green emission band and this emission arises from the defects in NiO/NiO:Zn lattice.When increasing the dopant concentration, intensity of the emission decreases compared to the undoped, it reflects the dislocation density value calculated from XRD data. From the PL graph it is concluded that the light emitting properties of synthesized samples have been used in green emission optoelectronic devices. Sheena *et. al*., [22] has observed similar type of PL spectrum

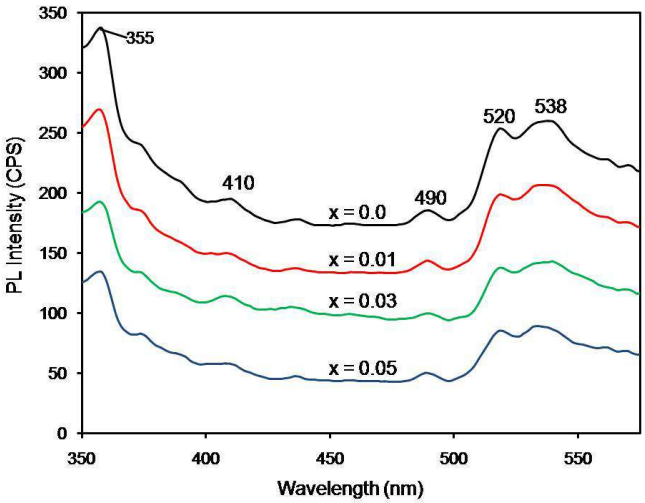

Figure 5. Room temperature PL spectrum of $Ni_{1-x}Zn_xO$ (x= 0, 0.01, 0.03, and 0.05) nanopowders

Microstructural and Compositional analysis

Size and surface morphology of the undoped and Zn doped NiO nanoparticles were examined by high resolution scanning electron microscopy (HRSEM) and the result is displayed in figure 6(a-c). The figure reveals that NiO particles having uniform size of 7 nm nanoparticles with severe aggregation. When doping Zn concentration is increased, the particle size also increases to 11 nm. In addition, the morphology of the particles transformed to rod-like structure as the Zn concentration is further increased to 5(wt%). The surface of the particles appears less homogeneous on higher concentration. The particle size estimated with HRSEM is less than the grain size value of XRD result. As the particle size is of the order of 10 nm, *i.e.*, *quantum dots*, it results in agglomeration. To confirm the particle size, we performed the TEM analysis.

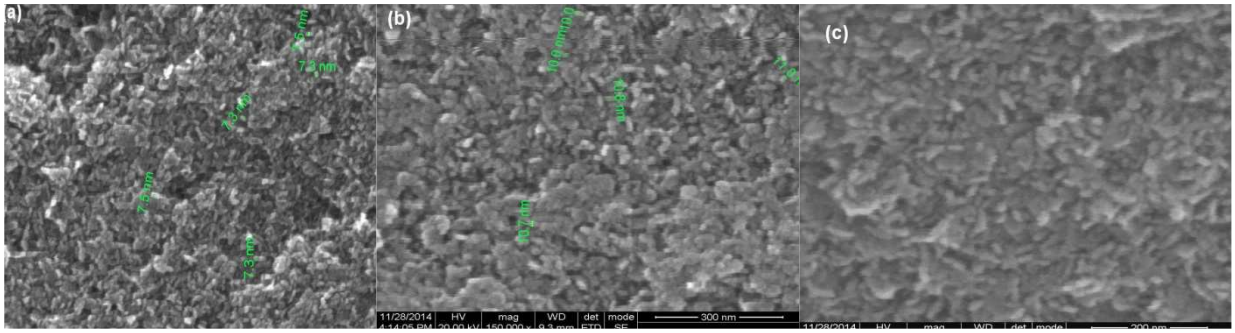

Figure 6. HRSEM images of (a) NiO, (b) $Ni_{0.99}Zn_{0.01}O$, and (c) $Ni_{0.97}Zn_{0.03}O$ nanopowders

Figure 7 is a typical TEM image of undoped NiO nanoparticles. As seen, the sample consists of very fine spherical particles with some nanorods. This kind of microstructure was also observed previously for NiO/NiO:Fe nanoparticles systems [23].

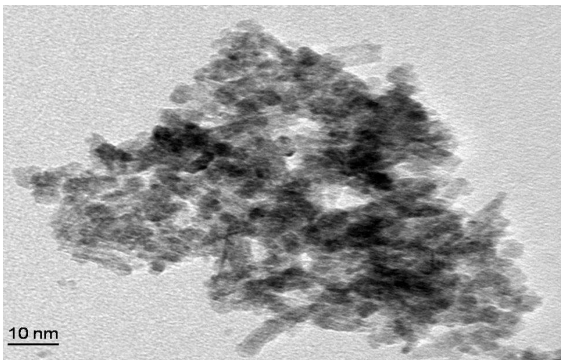

Figure 7. TEM image of $Ni_{0.95}Zn_{0.05}O$ powder

Figure 8 (a&b) shows the typical Energy Dispersive X-Ray Spectroscopy (EDS) spectra of the NiO and $Ni_{0.95}Ze_{0.05}O$ nanocrystalline particles, respectively. It is clear from the images that the undoped sample contains only Ni and O elements while the Ni and Zn elements are present in the Zn doped sample which confirms the successful doping of Zn in the NiO host structure and purity of the samples. The Zn concentration in the above mentioned $Ni_{0.95}Ze_{0.05}O$ sample is found to be 3.48%. Result of EDS analysis is shown in the inset of the respective figures.

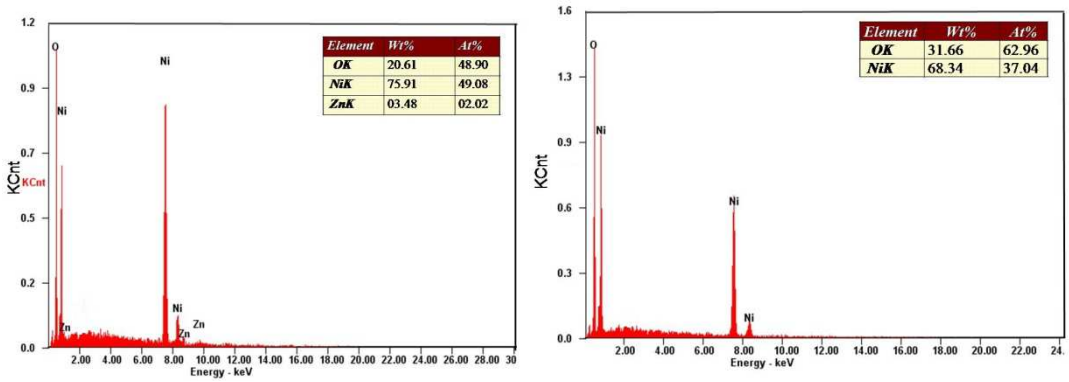

Figure 8. EDS analysis of NiO (Left), $Ni_{0.95}Zn_{0.05}O$ (Right) nanopowders

Thermo gravimetric analysis

Figure 9 shows the result of thermo gravimetric analysis (TG) and differential thermal analysis (DTA) curve for undoped and 5wt% Zn doped NiO sample, which was carried out from the ambient temperature to 700ºC in presence of N_2 atmosphere to study the thermal stability [24]. Weight losses were observed at different temperatures. The first weight loss 8% for undoped and Zn doped NiO were recorded around 120 ºC which is due to the evaporation of the water molecules and moisture of product. Second weight loss (22%) recorded between 120ºC and 240ºC is attributed to NO_2 and mixture of nickel nitrate. At the same time the combustion of Zn organic compound is the main reaction of the weight loss due to the dopant concentration. The sharp peaks at 250ºC for undoped NiO and Zn doped NiO are evidence of exothermic peak. Third weight loss (7%) occurred between 240ºC to 335ºC is associated with the decomposition of $Ni(OH)_2$. Final weight loss occurs around 335ºC - 400ºC.This stage is identified as complete crystallization of NiO and Zn doped NiO nanoparticles. Based on the TG& DTA result, it is confirmed that undoped and Zn doped NiO nanoparticles have the slightly changes in same thermal stability.

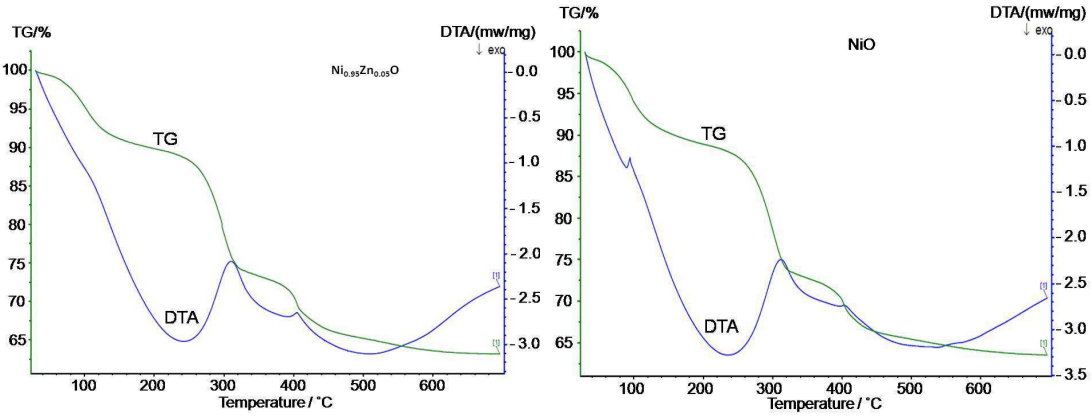

Figure 9.TG - DSC curve of NiO, $Ni_{0.95}Zn_{0.05}O$ nanopowders

Dielectric analysis

According to the theory, the dielectric behaviors of the nanomaterials are mainly due to different types of polarizations present in the material [25]. In the present work, we have studied the dielectric properties of undoped NiO and 5(wt%) Zn doped NiO investigated using LCR Hitester impedance meter. For this study, we measured the dielectric loss (tanθ) at different frequency and temperature**.** Temperature dependant dielectric loss of undoped and Zn doped NiO nanoparticles are shown in Figure10 (a & b). It is clearly observed that the dielectric loss of undoped NiO is high at lower temperature and it goes down with frequency, irrespective of the temperature.

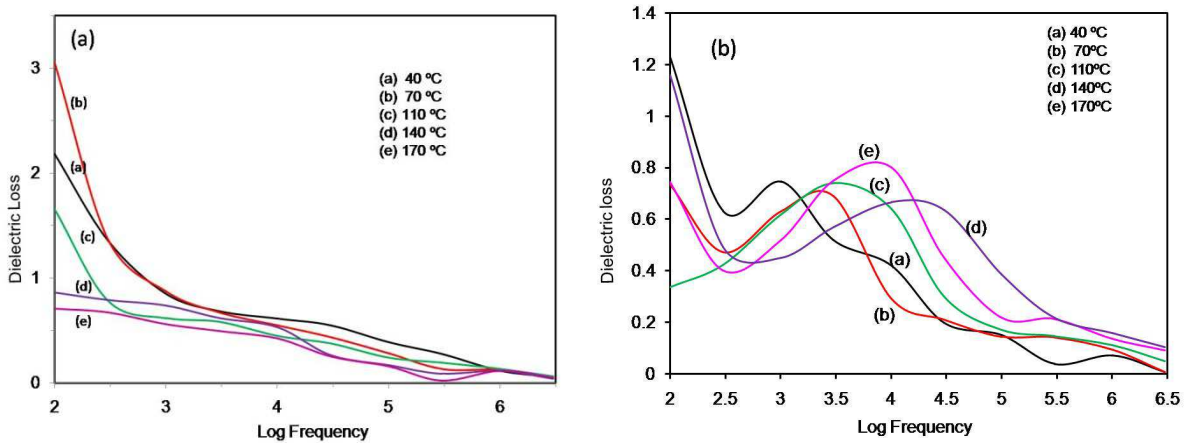

Figure 10. Dielectric constant vs. Log frequency of (a) undoped NiO. (b) $Ni_{0.95}Zn_{0.05}O$ nanoparticles

For the case of $Ni_{0.95}Zn_{0.05}O$ sample, initially dielectric loss decreases till the log frequency 2 thereafter it reaches maximum at log frequency 4. At this particular frequency, dielectric loss is maximum at 140˚C then it decreases as usually. Therefore, the dielectric loss study infers that the dielectric loss of NiO having a homogeneous response for all temperature and frequency whereas Zn doped NiO sample has slight changes in all the temperature and frequency.

CONCLUSION

In conclusion, NiO and Zn doped NiO nanoparticles have been successfully synthesized by chemical precipitation method. The XRD result confirmed that the prepared samples have FCC structure and the average grain size increases with Zn concentration. This result is also confirmed by HR-SEM and TEM analysis. UV– Visible result confirmed the energy gap of the synthesized nanoparticles is less than that of bulk NiO which in turn confirms the quantum confinement effect. The functional group identified from FTIR result confirmed the formation of NiO and Zn doping. Dielectric analysis confirmed that Zn doping increases the dielectric loss at high frequency. As a final point, it is concluded from the PL studies, that the Zn doped NiO nanoparticles can be used in green emission optoelectric devices.

Acknowledgements
The authors would like to thank SAIF, IITM Chennai for providing the HESEM and TG/DSC facilities and STIC-Cochin for TEM analysis.

REFERENCES

[1] S Kanchana; M Jay Chithra; S Suhashini Ernest; K Pushpanathan, *J. Lumin.*, **2016,** *176*, 6–14.
[2] M Jay Chithra; M Sathya; K Pushpanathan, *Acta. Metall. Sin. (Engl. Lett.).*, **2015**, *28*, 394 – 404.
[3] K Anandan; V Rajendran, *Nanosci. Nanotech.*, **2012,** *2*, 24-29.
[4] C Thangamani; K Pushpanathan, *J. Chem. Pharm. Sci.*, **2015,** 111-113.
[5] J Wang; JLWei; LL Zhang; LJ Zhang; H Wei; C Jiang; Y Zhang, *J. Matter Chem*. **2012**, *22*, 20038-20047.
[6] R Master; M Karandikar; A Jambhale; KD Tarachand Shukla; RJ Choudhary; MD Phase, *J. Phys. Conference Series*, **2014,** 534, 012025.
[7] S Thota; J Kumar, *J. Phys. Chem. Solids*., 2007, *68*, 1951-1964.
[8] J Wu; CW Nan;Y Lin; Y Deng, *Phys.Rev.Lett*. **2002,** *89*, 217601.
[9] JE Keem; JM Honig; LL Van Zandt, *Philos.Mag.B*, **1798**, *37*, 537-543.
[10] K Sathishkumar; N Shanmugam; N Kanndasan; S Cholan; G Viruthagiri, *Mater. Sci. Semicond. Processing*, **2014**, *27*, 846-853.
[11] K Karthi; G Kalaiselvan; M Kanagaraj; S Arumugam; N Victor Jaya, *J. Alloys Comps*., **2011**, *509*, 181-184.
[12] B Gokul; P Matheswaran; K M Abhirami; R Sathyamoorthy, *J. Non-Crystalline Solids.*, **2013,** *363*, 161-166.
[13] P Marlick; C Rath; R Biswal; NC Miahra, *Indian . J. Phys* ., **2009,** 83, 4.
[14] R Ramasubba Reddy; GS Harish; Ch Seshendra Reddy; P Sreedhara Reddy, *Inter. J. Modern Engg. Research*, **2014,** *4*, 62-66.
[15] P Mallick; NC Mishra, *American .J. Mater. Sci*., **2012,** *2*, 66-71.
[16] K Pushpanathan; S Sathya; M Jay Chithra; S Gowthami; R.Santhi, *Mater. Manufac. Proc*., **2012**, *27*, 1-9.
[17] BD Cullity, Elements of X-ray diffraction, 2nd edition. (Addison- Wesley Publishing Co., Inc., Reading, MA, USA, **1978**) p. 102.
[18] CT Meneses; WH Flores; F Garcia; JM Sasaki, *J. Nanoparticle Research.*, 2007, *9*, 501–505.

[19] G Bharathy, P Raji, International J.Chem Tech Research., **2014-2015**, 7, 1559-1562.
[20] M Nowsath Rifaya; T Theivasanthi; M. Alagar, *Nanosci. Nanotech*., **2012**, *2*, 134-138.
[21] NJ Tharayil; R Raveendran; AV Vaidyan; PG Chithra, *Indian J. Engg. Mater. Sci.* **2008**., *15*, 489-496.
[22] KP Priyanka; NA Sabu; PA Sheena; S Sreeja; T Varghese, *Nanosystems:Physics, Chemistry,Mathematics,*. ***2014***, *5 .441-449.*
[23] KO Moura; RJS Lima; CBR Jesus; JGS Duque; CT Meneses, *Revista Mexicana de F´ısica* S., **2012**, *58 (2)* 167–170.
[24] M Liu; Y Wang; P Li; Z Cheng; Y Zhang; M Zhang; M Hu; Li, *J. Appl. Surf. Sci*. **2013.**, *2609*, 2-6.
[25] PP Dorneanu; A Airinei; N Olaru; V Homocianu; V Nica; F Doroftei, *Mater. Chem. Phys.*, **2014**, *148,* 1029-1035.